A METHODOLOGY TO ASSESS ROBUST STABILITY OF AUTOMATIC FLIGHT CONTROL SYSTEMS

Alex Sander Ferreira da Silva, sander.silva@embraer.com.br
Henrique Mohallem Paiva, henrique.paiva@embraer.com.br
Sistemas de Comandos de Vôo, Empresa Brasileira de Aeronáutica - EMBRAER, Av. Brigadeiro Faria Lima 2170 - São José dos Campos - SP - 12227-901 - Brazil

Karl Heinz Kienitz, kienitz@ita.br
Divisão de Engenharia Eletrônica, Instituto Tecnológico de Aeronáutica - ITA, CTA - Praça Marechal Eduardo Gomes 50 - São José dos Campos - SP - 12228-900 - Brazil

Abstract. *Efficient development of automatic flight controls systems (AFCS) is mostly a model-based activity. Generally speaking, the better the quality of the models, in terms of representing the actual system, the better is the result that can be achieved. Nevertheless, it is always necessary to consider that models are not perfect, in the sense that there is normally a part of the real system dynamics which is either not well represented or deliberately neglected. This paper proposes a methodology to assess the robust stability of AFCS using the structured singular value, μ. For means of comparison, an approach widely used in the aircraft industry to measure the stability of AFCS is reviewed and its issues are discussed. A case study is presented, showing that the proposed method is an elegant alternative and deals conveniently with the drawbacks of the quoted industrial technique.*

Keywords: *Robust Control, Structured Singular Value, Feedback Systems, AFCS*

1. INTRODUCTION

Modern automatic flight controls systems (AFCS) design and analysis is a model-based activity. This means that, in a preliminary step, it is necessary to develop aircraft models as well as the models of the aircraft main peripherals, like actuators, engines, etc. Modeling comprises a vast engineering area and its detailed discussion lies beyond the scope of this paper. Fortunately there is an extensive and rich literature presenting the main aspects of aircraft modeling (Stevens; Lewis, 1992; Mcruer et al., 1973; Mclean, 1990; Babister, 1961; Dommash et al., 1967; Millikan, 1958).

One important output of the modeling activity is the understanding of the possible inaccuracies that might be present in the particular model under study. This knowledge can be used during the design phase in order to minimize the possibility of AFCS rework during the final flight test phase, since it is well known that major changes during this stage are time consuming and expensive.

Broadly speaking, the robustness stability assessment consists in verifying if the required stability is maintained, considering all possible plant variations within their assumed bounds. Such verification does not depend on the particular choice of the AFCS design synthesis technique. In fact, they can even be used as judgment criteria of the quality of a specific AFCS controller.

Since having reliable measures of control law robust stability is an unquestionable necessity, flight control law designers keep a constant interest on the subject. This article revisits one of the largely used procedures to check robust stability of AFCS and points out its limitations. The subsequent focus is to show how the concept of structured singular value can be used to fill in the existing gaps. The final goal is to provide a step by step methodology which incorporates the advantages offered by the currently used method and also makes use of μ to eliminate its weaknesses.

The text is organized as follows. Section 2 presents a general layout, applicable to a broad class of AFCS control laws. It also identifies the AFCS elements responsible in guaranteeing robustness. Section 3 provides a short description of one particular AFCS. It also presents the aircraft models, valid for one flight condition, as well as the adopted modeling of the flight controls elements. Section 4 discusses a method widely used in the aircraft industry to assess AFCS robust stability. Section 5 provides the add-ons sufficient to overcome the present limitations of the method from Section 4. The analysis plots provided in Section 4 and 5 are based on the models described in Section 3. Final remarks are given in Section 6.

2. AFCS GENERAL LAYOUT

The model arrangement depicted in Fig.1 shows the links encountered in a general AFCS application (Aircraft, Sensors, Actuators, flight control computer, Pilot, etc). Aircraft dynamics is represented by the multiple inputs multiple outputs (MIMO) system, having as inputs $U_1, U_2, \ldots, U_p$ and as outputs the signals $In_1, In_2, In_3, \ldots, In_n$. The sensors dynamics are located inside the block *Sensor Models*.

The AFCS control law uses the measured signals, S_n, and the reference signals, R_t, which are provided either by the pilot or by the navigation computer. The control algorithm provides the demands for the aircraft inputs, $ComU_p$.

Pure time delays, representing either the data transportation on digital buses or the computer calculation lag, are also implemented inside the block *AFCS*.

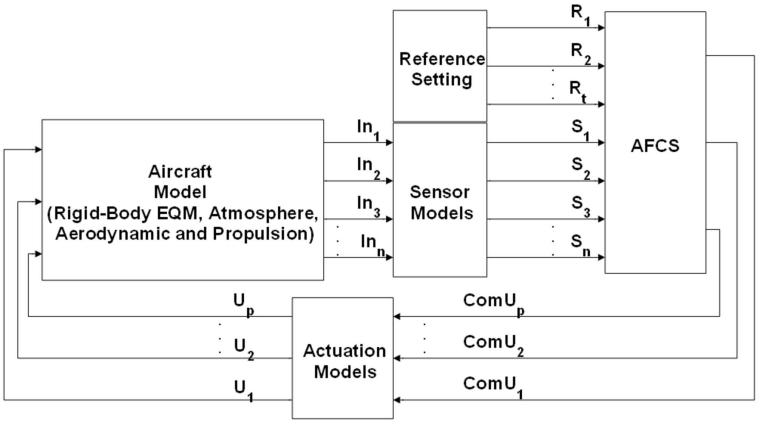

Figure 1. Model Arrangement - Overview

Figure 2 shows a general AFCS layout. The signal pre-processing block computes the signals estimate to be used on the control law. It takes the available measurement from the aircraft sensors and performs data computation and filtering. The Set-Point Generator computes the feedback set-points, based on either the pilot or navigation computer inputs and, finally, the feedback section computes the aircraft inputs demands based on the error between the estimated variable and the respective set-point.

The sensed signals used by the control algorithm, S_{nd}, is the delayed version of the sensors output. This delay is due to the transport delay inherent of digital buses. The aircraft input demands produced by the control law, $ComU_{pu}$, also suffer a delay prior to reaching the actuators.

The control strategy encapsulated in Fig. 2 is a two degree of freedom control law structure (Kreisselmeier, 1999). Two major responsibilities shall be addressed by the subsystem containing the feedback component and the data pre-processing, namely the disturbance rejection and the assurance of overall system robustness. It means that these are the elements which are tested during the robustness checks.

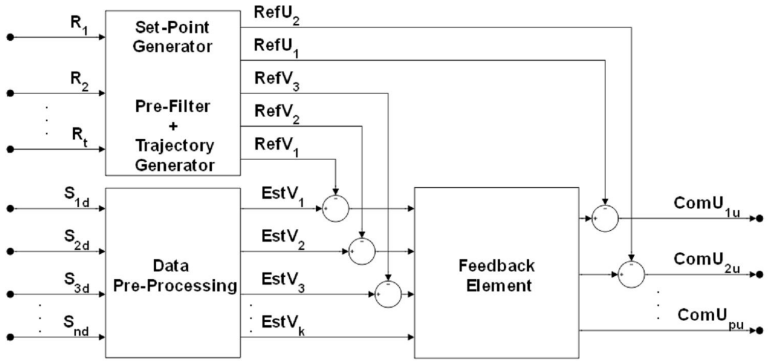

Figure 2. AFCS General Structure

3. SHORT DESCRIPTION OF ONE SPECIFIC AFCS

The AFCS which is presented in this Section is an example of a ψ hold/ψ capture control law. In other words, this is an auto pilot function which holds the desired heading and also allows the proper transitions from one initial heading to the final one.

Another function of this AFCS is the regulation of the side slip angle, β, around zero. This is important for two basic reasons: 1 - This is what damps out the aircraft's Dutch roll mode. 2 - One regulator of β, instead of a simple regulator of $\dot{\beta}$, which comprises the conventional *Yaw damper* of commercial aircraft, additionally provides the automatic trimming of the aircraft's lateral axis.

The objective is not to present how this final design was achieved. The goal is to provide a design, with performance compatible with a good auto pilot, and then use it to aid in the presentation of the methods described in Sections 4 and 5.

3.1 Aircraft Dynamics

Based on the information presented in (Hanke, 1971; Hanke; Nordwall, 1970; Heffley; Jewell, 1972), a non-linear model of the Boeing 747 aircraft was assembled using Simulink/Matlab.

Together with the model, a series of Matlab scripts was prepared to automate the routines necessary for the design and analysis of flight control laws. Two of these functions perform the trimming and the linearization around the trimming condition.

The analysis on Sections 4 and 5 are based on two linear latero-directional models. These represent the two extreme mass configurations available in one flight condition. Table 1 presents the flight condition, together with the description of the mass configurations.

Table 1. Linear Models - Flight Condition and Mass Configurations

Case	**Mass** [kg]	$\mathbf{CG}_{POS}$ $^{(1)}$ [%]	$\mathbf{V}_{CAS}$ [kn]	$\mathbf{h}_p$ [ft]
Model 1	181440	25	244	20000
Model 2	317510	25	244	20000

$^{(1)}$: Center of gravity position, in the longitudinal axis

The linear aircraft models have aileron and rudder position as inputs and side slip angle (β), bank angle (ϕ), roll rate (p), yaw rate (r), lateral acceleration at the center of gravity location (A_YCG) and heading (ψ) as outputs.

3.2 Sensor Models

The output of each sensor carries not only the aircraft specific parameter dynamics, but also has some spurious dynamics due to the sensing device itself. The lesser the contamination of the data with the sensor dynamics, as well as with sensor noise, the better is the specific sensor signal.

In this study, the sensors are modeled as a second order lag plus one pure time delay. For linear analysis purpose, the pure time delays are replaced by second order Padé approximation (Stevens; Lewis, 1992). Table 2 presents the chosen values of the second order lag natural frequency (ω_n), the associated poles damping ratio (ζ) and the pure time delay values.

Table 2. Sensor dynamics Values

Sensed Signal	ψ	ϕ	p	r	A_{YCG}	β
Time Delay [ms]	20	20	10	10	10	20
ω_n $[rad/s]$	94.2	94.2	75.4	75.4	50.3	12.0
ζ	1.0	1.0	1.0	1.0	1.0	0.7

3.3 Actuation Models

A practical AFCS design must also take into account the limitations imposed by the actuation system. This system can be mathematically described by an input-output relationship between the intended and actual positions.

In this study, the actuators are modeled as a second order lag. Table 3 presents the chosen values of the second order lag natural frequency (ω_n), the associated poles damping ratio (ζ) and the actuator steady state gain (K).

Table 3. Actuation system Values

Input	K	ω_n $[rad/s]$	ζ
Aileron	1	31.4	0.7
Rudder	1	31.4	0.7

3.4 AFCS Computer

At the present time, the flight control laws are almost invariably implemented in digital computers. The primary advantage in following this approach is the flexibility in executing complex data manipulations.

One shortcoming is the pure time delay which is added due to the nature of digital calculations. Nevertheless, this drawback is of secondary order today and it tends to become meaningfulness in the future, as the computer capacity is rapidly increasing.

Table 4 presents the chosen transport delays from sensor to the AFCS computer. In real application, these values are dictated by the priority assigned for each signal, given the limitation imposed by the capacity of the particular digital bus used.

Table 4. Transport delay from Sensor to AFCS computer

Sensed Signal	ψ	ϕ	p	r	A_{YCG}	β
Transport Delay [ms]	20	20	10	10	10	20

The computation lag is represented by a 25 ms delay, added at the output of the control law algorithm. Since the control laws are digitally implemented, the effects of the sampler plus the zero order hold (ZOH) must also be accounted for.

For linear analysis purpose, the pure time delay is replaced by a second order Padé approximation, while the ZOH is replaced by a first order approximation. These approximations can be found in (Stevens; Lewis, 1992).

3.5 AFCS Function

The objective of this subsection is to provide some additional information on how this specific AFCS (ψ hold/ψ capture) works. It also provides evidences that this studied design has a performance compatible with one good Auto Pilot (AP).

This AFCS uses aileron and rudder to control the ψ and β. Figure 3 (a) shows the time history for one ψ transition, from 0 deg to 60 deg. The pilot input is represented by the ψ_{SEL} curve, which is the output of a ψ knob, located in the cockpit. The ψ_{CMD} is the set-point on ψ, which is generated based on the ψ_{SEL} signal. The ϕ_{Cmd} is the set-point on bank-angle. This signal is the command sent by the *outer loop* to the *inner loop*.

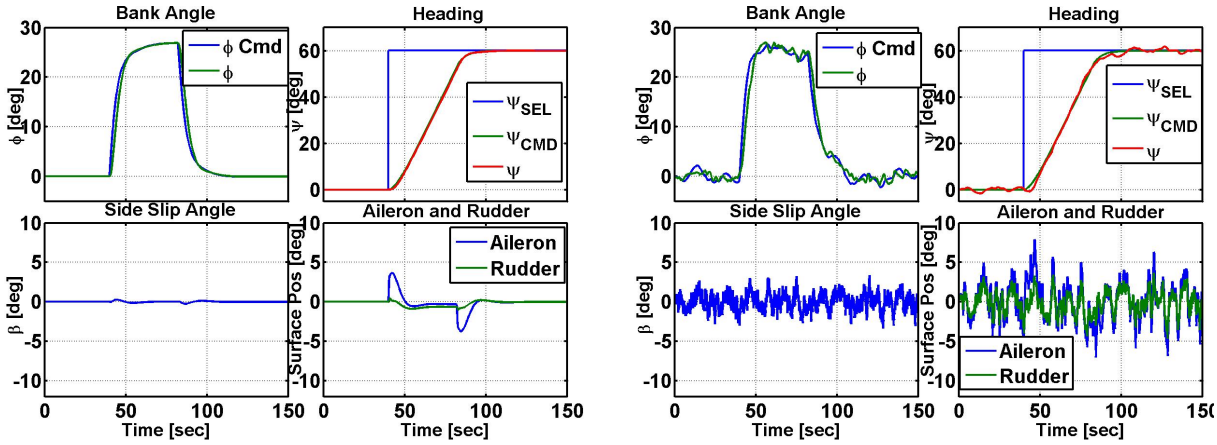

Figure 3. Time History - ψ transition and ψ hold

The plots in Fig. 3 (a) were generated considering model 1 (see Tab. 1) and atmospheric conditions without any turbulence. Figure 3 (b) refers to the same model, but now including severe turbulence level. The turbulence modeling is based on (DoD, 1990). Similar results are achieved when using model 2 of Tab. 1.

The basic conclusion from these plots is that this control law is able of performing the ψ transition as well as the ψ hold in a desired fashion, even when the *strongest* possible turbulence level is included.

4. CURRENT INDUSTRIAL METHOD TO ASSESS ROBUSTNESS

In order to help out in the subsequent explanations, the following definition, valid in the context of this work, is introduced:

Open Loop Transfer Function($OLTF$): It is the single input single output (SISO) system obtained after the closed loop system is opened at one control law designated location. The particular point where this procedure is carried out can be one of the following: 1 - Any sensor input used by the control law. 2 - Any of the aircraft inputs used by the control law. 3 - Any internal point of the control law block diagram. The abbreviation $OLTF_{In_2}$ denotes open loop transfer function at the signal In_2, as illustrated in Fig. 4.

An AFCS control law is said to possess robust stability if the OLTF of every one of the inputs to the *sensor models* ($OLTF_{In_1}, \ldots, OLTF_{In_n}$), as well as the OLTF of the aircraft inputs used by the control law ($OLTF_{U_1}, \ldots, OLTF_{U_p}$),

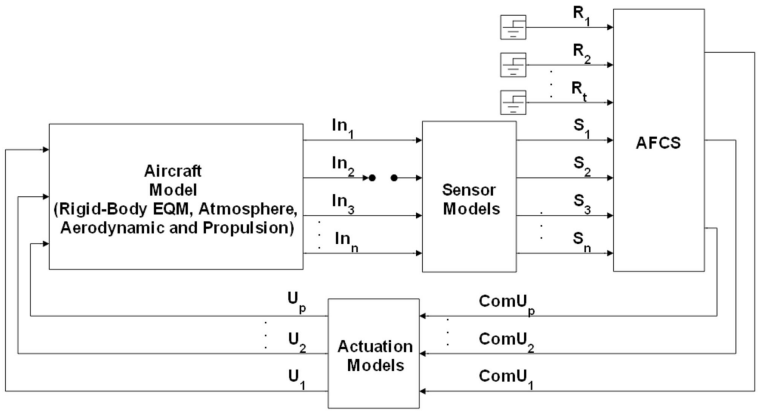

Figure 4. Illustration of the building up of one OLTF

have certain characteristics.

The quoted characteristics are extracted from the Magnitude versus Phase plot of the -OLTF. The test consists in a graphical check of these transfer functions against a pre-defined template, which can be modified in accordance with the problem in hand.

Figure 5 (a) presents one example of a case which passes the robustness criterion, while Fig. 5 (b) presents a failed one. The red curve is the edge, constructed around the critical point, marking the so called *robustness boundary*. In this case, it is used straight lines connecting the $\pm$ 6 db gain margin with the $\pm$ 45 degrees phase margin points. These values, as well as the shape of this boundary, can be modified, without effect on the following discussion.

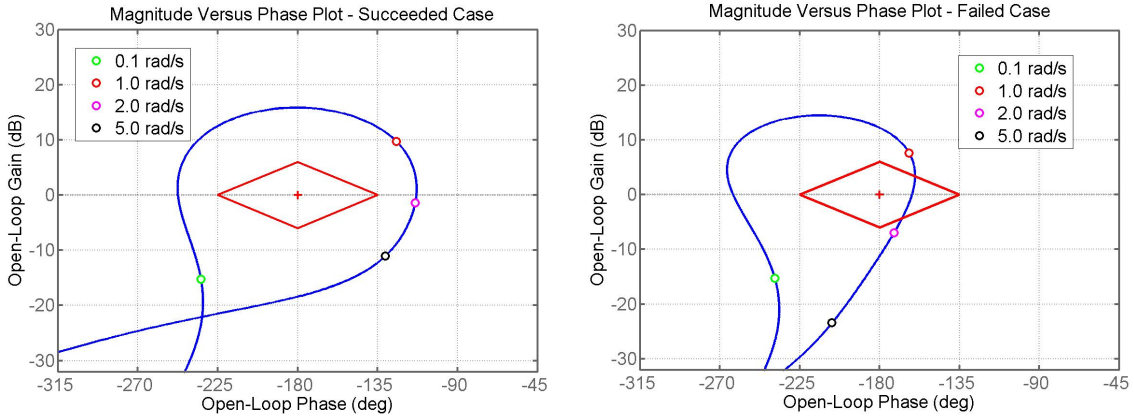

(a) (b)

Figure 5. Magnitude Versus Phase Plot - Success and Failed in the Robustness test

As already mentioned, the just presented robustness check consists in a widespread procedure employed in the aircraft industry. Examples of similar robustness check methodology can be found in (Garteur, 1996; Gangsaas et al., 2008). Nevertheless, there are issues on this method, which are discussed in the sequence.

The basic concept behind this process is the Nyquist Stability Criterion (Ogata, 1997), applied to SISO systems. The *robustness boundary* is set as the region, around the critical point, which shall be avoided. The further is the magnitude versus phase plot of the $-OLTF$ to the critical point the more robust is the closed loop system.

This concept, which has roots in gain and phase margin check, is a powerful tool, which can be readily applied to any SISO system. Applying this to the described $OLTFs$, extracted out from a MIMO system, is an extrapolation which can present issues (Skogestad; Postlethwaite, 2001). Problems may arise since this concept assumes that each loop is modified without any perturbation on the other loops. One particular example where this assumption is valid is the case where there is either an unknown scale factor or an unknown additional time delay applied to only one of the sensors signals. However, this assumption is not valid in the general case, because a model inaccuracy may affect all the loops.

One approach to minimize the concerns just described above consists in checking the $OLTF$ of the extremes of the mass and CG envelope, for the given flight condition. The idea is to make sure that the same level of margins is kept, regardless of the mass configuration under study. This practice adds mores confidence on the robustness test, since not only one nominal model is checked, instead, one set of models, representative of the mass and CG envelope is tested

simultaneously.

Nonetheless, no mathematical certainty can be given by this approach. One elegant procedure to bypass this weakness can be achieved by using the structured singular value, called here μ_Δ.

Figure 6 provides the magnitude versus phase plots of the ψ hold/ψ capture control law. The two curves on each plot represent the two mass configurations of Tab. 1.

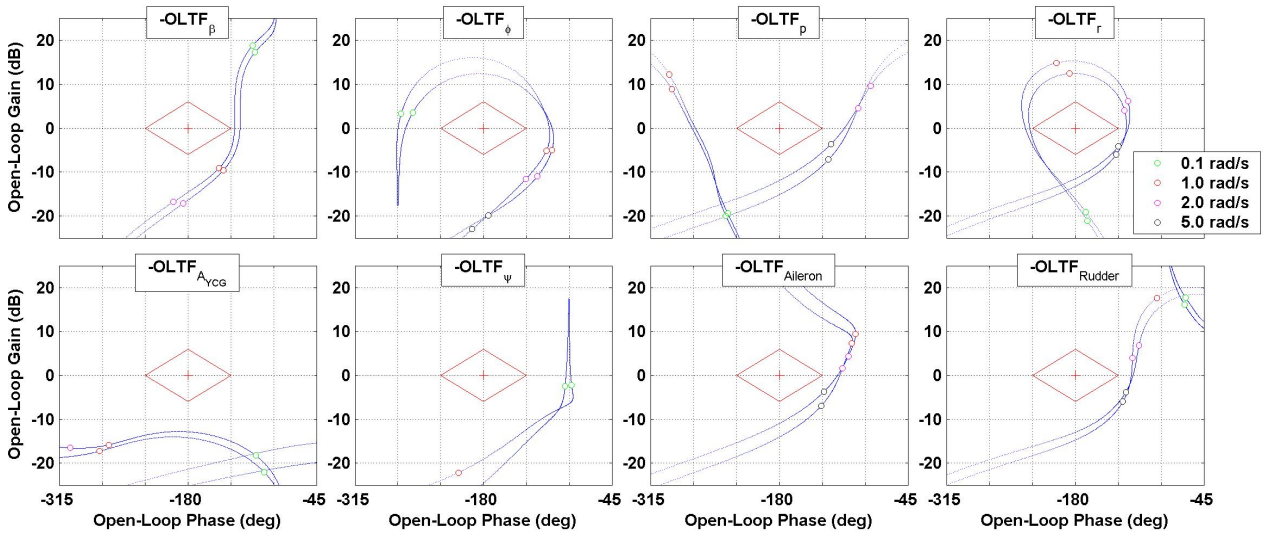

Figure 6. Magnitude Versus Phase Plot - ψ hold/ψ capture control law

5. COMPLETING THE ROBUSTNESS TEST

There is an extensive amount of publications about μ (Looye et al., 1998; Skogestad; Postlethwaite, 2001; Balas et al., 2001; Doyle, 1982). The objective of this Section is not to provide any new theory on this mathematical entity. On the other hand, the intention is to make use of the well established characteristics of this tool, with the final target of setting one set of tests to measure the robust stability.

It is first provided a short review of μ. The related terminologies, which are used in this work, are introduced in this stage. The subsequent step is the definition of the quoted robustness tests. For the purpose of giving one example, the defined tests are then applied on the ψ hold/ψ capture control law.

5.1 Short review of μ

The starting point for the robustness analysis is a system representation in which the uncertain perturbations are lumped into a block diagonal matrix, see Eq. (1).

$$\Delta = diag\{\Delta_i\} \tag{1}$$

When following this approach, the control problem can be stated in terms of the general formulation (Doyle, 1983; Doyle, 1984). For the particular case of control law robust stability analysis, it is sufficient to use the $M\Delta-$Structure (Skogestad; Postlethwaite, 2001) depicted in Fig. 7.

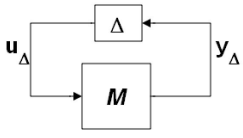

Figure 7. $M\Delta-$Structure for robust stability analysis

Where M is the generalized plant, including the controller and the perturbations weight on it. The Δ matrix, representing the system perturbations, is built in a way to satisfy $\|\Delta\|_\infty \leq 1$.

The definition of the structured singular value of a complex matrix M, for the allowed structure Δ, is presented on Eq. (2).

$$\mu\left(M\right)^{-1} \triangleq \min\left\{\bar{\sigma}\left(\Delta\right) | \det\left(I - M\Delta\right) = 0 \quad for\, structured\, \Delta\right\} \tag{2}$$

Clearly $\mu(M)$ depends not only on M, but also on the allowed structure for Δ. For this reason, it is preferable to use the notation $\mu_{\Delta}(M)$. In words, $\mu_{\Delta}(M)$ is the reciprocal of the smallest structured Δ (with $\bar{\sigma}$ as the norm) that can be found and that can makes the matrix $I - M\Delta$ singular.

Based on the terms defined on this Section, it possible to formulate the robust stability (RS) in terms of the conditions stated on Eq. (3) (Skogestad; Postlethwaite, 2001).

$$RS \Leftrightarrow \mu_{\Delta}(M) < 1,\ \forall\omega,\ and\ NS\ satisfied \tag{3}$$

Where NS means nominal stability, which is verified by the simple verification of all the closed loops poles real part.

5.2 Proposed tests based on μ

The uncertainty in the control system can be placed into the structure of Fig. 7 by considering that each input and output of the aircraft is subjected to scale factor and phase type inaccuracies. This is achieved by following the approach described below:

1. Add the perturbation weight described in Fig. 8 (a) for all the aircraft outputs which has phase type inaccuracy. The value of τ_{delay} represents the maximum expected additional delay, in seconds, that might be present on the particular signal;
2. Add the perturbation weight described in Fig. 8 (b) for all the aircraft outputs which has scale factor type inaccuracy. The value of f_{Signal} represents the maximum expected scale factor that might be present on the particular signal;
3. Repeat items number 1 and 2, but now for all of the aircraft inputs.

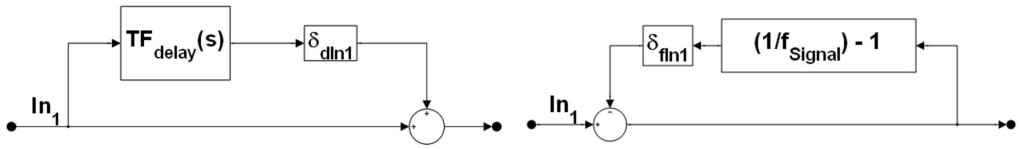

(a) (b)

Figure 8. Perturbation due to delay inaccuracy and scale factor inaccuracy

The transfer function $TF_{delay}(s)$ has the general format as described in Eq. (4)(Skogestad; Postlethwaite, 2001).

$$TF_{delay}(s) = \frac{\tau_{delay} s}{\frac{\tau_{delay}}{2} s + 1} \times \frac{\left(\frac{\tau_{delay}}{2.363}\right)^2 s^2 + 2 \times 0.838 \times \left(\frac{\tau_{delay}}{2.363}\right) s + 1}{\left(\frac{\tau_{delay}}{2.363}\right)^2 s^2 + 2 \times 0.685 \times \left(\frac{\tau_{delay}}{2.363}\right) s + 1} \tag{4}$$

In Fig. 8, δ_{dIn1} represents an uncertain complex gain and δ_{fIn1} represents an uncertain real gain. The magnitudes of both δ_{dIn1} and δ_{fIn1} are limited to be less than or equal to 1.

For the particular case where it is assumed the existence of inaccuracy in only one loop, it can be shown that the result of RS via μ provides the same conclusion as the OLTF phase and gain margin check. As an example of this feature, figure 9 (a) shows the magnitude versus phase plot of the $-OLTF_{\phi}$, where it is shown a phase margin of 69.2 deg at 0.58 rad/s, corresponding to an equivalent delay margin of 2.07 sec. Figure 9 (b) shows the $\mu_{\Delta}(M)$, considering that the only source uncertainty is a delay inaccuracy on the ϕ loop and that the maximum expected inaccuracy corresponds to $T_{Signal} = 2.07sec$. The plot of $\mu_{\Delta}(M)$ crosses 1 at the phase margin frequency provided by the $-OLTF_{\phi}$ plot.

Similar results are achieved considering phase perturbations on the other loops, as well as gain factor perturbations. Therefore, when it is considered inaccuracy in only one loop at each time, the conclusion based on the μ analysis produces the same result as the margins checks of the $OLTF$. However, the μ analysis allows the additional check of simultaneous perturbations in a straightforward manner.

5.3 Results of ψ hold/ψ capture control law

In order to exercise the concepts presented in this Section, the ψ hold/ψ capture controls law is tested, considering the maximum model inaccuracies as described on Tab. 5.

The final results are shown in Fig. 10. One important note is that the μ_{Δ} plots shown on this article is in fact an upper bound on the respective μ_{Δ}.

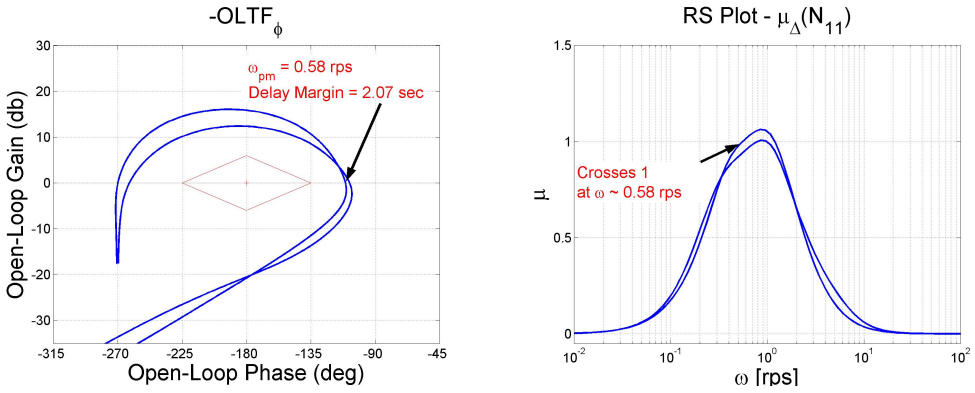

(a) (b)

Figure 9. Confirmation of the robustness test based on μ

Table 5. Model inaccuracy factors

Signal	ψ	ϕ	p	r	A_{YCG}	β	Aileron	Rudder
τ_{delay} [s]	0.020	0.020	0.010	0.010	0.010	0.020	0.010	0.010
f_{Signal} [ADM]	1.00	1.00	1.00	1.00	1.00	1.00	1.15	1.15

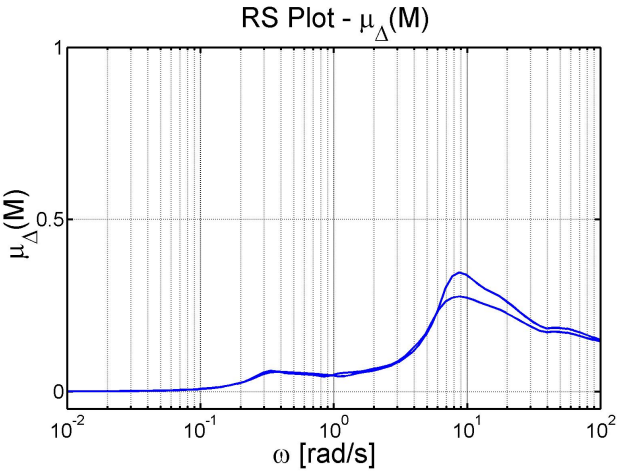

Figure 10. μ results

6. CONCLUSIONS

The proposed additional test, based on the concept of μ_Δ, allows the determination, in one go, of the worst combination of the possible errors, in terms of hampering the final stability. The current quoted method has the drawback of assuming that the model inaccuracy affects only one of the loops. This can be the case sometimes, but, in the general situation, there are possible inaccuracies in each of the aircraft inputs or sensor inputs. The actual modeling error can be the result of any of the possible combinations.

The proposed final procedure combines the two presented methodologies. The reason is that -OLTFs magnitude versus phase plot can be used not only as robustness measurement tool of individual loops uncertainty, but also as a instrument for guiding the control law loop shaping, obtained via phase shift and/or gain increase/decrease of the -OLTFs. One important result of the proper loop shaping of all the OLTF is linked with the fact that the damping of the closed loop poles are intimately linked with the proximity of these curves to the critical point.

The supplementary test, based on μ_Δ, works as a complement for the current methodology, since it fulfills the existing gap. It does not provides the same aid in terms of indicating the best strategy for loop shaping, but it provides the correct assurance of robust stability for the more common situation, where the errors may happen simultaneously in multiple loops.

7. REFERENCES

Babister, A. W., 1961, "Aircraft Stability and Control", Pergamon Press, New York, USA.

Balas, G. J. et al., 2001, "μ-Analysis and Synthesis TOOL-BOX, For Use with MATLAB", The MathWorks, Inc., Natick, USA.

Dommash, D. O.; Sherby, S. S.; Connolly, T. F., 1967, "Airplane Aerodynamics", Pitman Publishing Corporation, New York, USA.

DoD, 1990, "Flying Qualities of Piloted Aircraft", Military Standard MIL-STD-1797A.

Doyle, J. C., 1982, "Analysis of feedback systems with structured uncertanties", IEEE Proceedings, Part D 129(6), pp. $242 - 250$.

Doyle, J. C., 1983, "Synthesis of robust controllers and filters", Proc. IEEE conf. on Decision and Control, San Atonio, USA, pp. $109 - 114$.

Doyle, J. C., 1984, "Lecture Notes on Advances in Multivariable Control", ONR/Honeywell Workshop, Minneapolis, USA.

Gangsaas, D. et al., 2008, "Multidisciplinary control law design and flight test demonstration on a business jet", Paper AIAA 2008-6489, AIAA Guidance, Navigation and Control Conference and Exhibit, Honolulu, USA.

Garteur, 1996, "Robust Flight Control Design Challenge Problem Formulation and Manual: The High Incidence Research Model (HIRM)", GARTEUR/TP-088-4.

Hanke, C. R.; Nordwall, D. R., 1970, "The Simulation of a Jumbo Jet Transport Aircraft", Volume II: Modeling Data, Technical Report NASA-CR-114494, National Aeronautics and Space Administration, Washington, USA, 1970, available from http://ntrs.nasa.gov/search.jsp?N=4294913218 (last access February, 26, 2009).

Hanke, C. R., 1971, "The Simulation of a Large Jet Transport Aircraft", Volume I: Mathematical Model, Technical Report NASA-CR-1756, National Aeronautics and Space Administration, Washington, USA, 1971, available from http://ntrs.nasa.gov/search.jsp?N=4294913218 (last access February, 26, 2009).

Heffley, R. K.; Jewell, W. F, 1972, "Aircraft Handling Qualities data", Technical Report NASA-CR-2144, National Aeronautics and Space Administration, Washington, USA, 1972.

Kreisselmeier, G., 1999, "Two degree of freedom control", Automatisierungstechnik, Vol.47, n. 6, pp. $266 - 269$.

Looye, G. et al., 1998, "Robustness analysis applied to autopilot design, part 1: μ-analysis of design entries to a robust flight control benchmark", Proc. 21st Congress of the International Council of Aeronautical Sciences, 1998, available from http://elib.dlr.de/3454/01/looye_Icas98_1.pdf (last access February, 26, 2009).

Mclean, D., 1990, "Automatic Flight Control Systems", Prentice Hall, Cambridge, UK.

Mcruer, D.; Ashkenas, I.; Graham, D., 1973, "Aircraft Dynamics and Automatic Control", Princenton University Press, Princenton, New Jersey, USA.

Millikan, C. B., 1958, "Aerodynamics of the Airplane", John Wiley and Sons, Inc, New York, USA.

Ogata, K., 1997, "Modern Control Engineering", Prentice Hall, Upper Saddle River, New Jersey, USA.

Skogestad, S.; Postlethwaite,I., 2001, "MULTIVARIABLE FEEDBACK CONTROL – Analysis and Design", John Wiley and Sons, Inc., New York, USA.

Stevens, B. L.; Lewis, F. L., 1992, "Aircraft Control and Simulation", John Wiley and Sons, Inc., New York, USA.